REPRESENTATION OF THE EARTH'S GRAVITATIONAL POTENTIAL*

JOHN P. VINTI

MIT Measurement Systems Laboratory, Cambridge, Mass., 02139, U.S.A.

(Received 14 October, 1970)

Abstract. The paper represents the Earth's gravitational potential V, outside a sphere bounding the Earth, by means of its difference δV from the author's spheroidal potential. The difference δV is in turn represented as arising from a surface density σ on the sphere bounding the Earth. Because of the slow decrease with order n of the normalized coefficients in the spherical harmonic expansion of V, the density anomalies from which the higher coefficients arise must occur in regions close to the Earth's surface. The surface density σ is thus an idealization of the product of the density anomaly $\Delta\varrho$ and the crustal thickness b. Values of σ are computed from potential coefficients obtained from two sources, Rapp and the Smithsonian Astrophysical Observatory. The two sources give qualitative agreement for the values of σ and for its contour map. The numerical values obtained for σ are compatible with the idea that the responsible density anomalies are reasonably small, i.e., less than 0.05 g/cm^3, and occur in the crust alone.

1. Introduction

Outside a sphere enclosing the Earth, its gravitational potential V can be expressed as a series of spherical harmonics, which is known to converge. With origin at the Earth's center of mass, this series has the form

$$V = -\frac{\mu}{r}\left[1 - \sum_{n=2}^{\infty}\left(\frac{R}{r}\right)^n J_n P_n(\cos\theta) + \sum_{n=2}^{\infty}\left(\frac{R}{r}\right)^n \sum_{m=1}^{n} P_n^m(\cos\theta)\,(C_{n,m}\cos m\lambda + S_{n,m}\sin m\lambda)\right]. \tag{1}$$

Here $\mu \equiv GM$, the product of the gravitational constant and the mass of the Earth, R is a conventional equatorial radius, and r, θ, and λ are respectively the geocentric distance, colatitude, and longitude of a field point outside a sphere enclosing Mount Everest. $P_n(\xi)$ is the Legendre polynomial of ξ, of degree n, and $P_n^m(\xi) \equiv (1-\xi^2)^{m/2} \times \times \mathrm{d}^m P_n(\xi)/\mathrm{d}\xi^m$. The constants J_n are the zonal coefficients, the $C_{n,m}$ and $S_{n,m}$ are the tesseral coefficients if $1 \leqq m < n$ and the sectorial coefficients if $m = n$.

On writing

$$J_n = -\,C_{n,0}\,, \tag{2}$$

* This paper was prepared under the sponsorship of the Electronics Research Center of the National Aeronautics and Space Administration through NASA Grant NGR 22-009-311.

Celestial Mechanics **4** (1971) 348–367.

Equation (1) becomes

$$V = -\frac{\mu}{r}\left[1 + \sum_{n=2}^{\infty}\left(\frac{R}{r}\right)^n \sum_{m=0}^{n} P_n^m(\cos\theta)\,(C_{n,m}\cos m\lambda + S_{n,m}\sin m\lambda)\right], \tag{3}$$

where the $S_{n,0}$ may all be taken to be zero.

For large n, the quantities P_n^m may become large, especially if $m=n$, for which

$$P_n^n(\xi) = \frac{(2n)!}{2^n n!}(1-\xi^2)^{n/2}. \tag{4}$$

The corresponding C's and S's are accordingly very much smaller than the J's. To avoid the numerical inconvenience of multiplying very large numbers by very small numbers, it is now customary to normalize these tesseral and sectorial terms. Thus with the definition

$$\bar{P}_n^m \equiv \left[\frac{2(2n+1)(n-m)!}{(n+m)!}\right]^{1/2} P_n^m, \quad (m \geqq 1) \tag{5}$$

the tesserals and sectorials are 'normalized to 4π':

$$\int_0^{2\pi} d\lambda \int_0^{\pi} [\bar{P}_n^m(\cos\theta)]^2 \begin{Bmatrix}\cos^2 m\lambda \\ \sin^2 m\lambda\end{Bmatrix} \sin\theta\, d\theta = 4\pi. \tag{6}$$

Then, writing

$$\begin{Bmatrix}\bar{C}_{n,m} \\ \bar{S}_{n,m}\end{Bmatrix} \bar{P}_n^m = \begin{Bmatrix}C_{n,m} \\ S_{n,m}\end{Bmatrix} P_n^m, \tag{7}$$

we obtain

$$\begin{Bmatrix}\bar{C}_{n,m} \\ \bar{S}_{n,m}\end{Bmatrix} = \left[\frac{(n+m)!}{2(2n+1)(n-m)!}\right]^{1/2} \begin{Bmatrix}C_{n,m} \\ S_{n,m}\end{Bmatrix}. \tag{8}$$

To put the zonal harmonics into the same computer program with the tesserals it is convenient to normalize them also. With the definition

$$\bar{P}_n \equiv (2n+1)^{1/2} P_n, \tag{8.1}$$

we have

$$\int_0^{2\pi} d\lambda \int_0^{\pi} [\bar{P}_n(\cos\theta)]^2 \sin\theta\, d\theta = 4\pi, \tag{8.2}$$

as for the tesserals. Then with

$$\bar{C}_{n0}\bar{P}_n = C_n P_n, \tag{8.3}$$

we have

$$\bar{C}_{n0} = -\bar{J}_n = -(2n+1)^{-1/2} J_n. \tag{8.4}$$

With all harmonics normalized, the series becomes

$$V = -\frac{\mu}{r}\left[1 + \sum_{n=2}^{\infty}\left(\frac{R}{r}\right)^n \sum_{m=0}^{n} \bar{P}_n^m(\cos\theta)\,(\bar{C}_{n,m}\cos m\lambda + \bar{S}_{n,m}\sin m\lambda)\right]. \tag{9}$$

In this expansion $\bar{C}_{20} \approx -(484)\,10^{-6}$ and the higher coefficients are of order 10^{-6} for a number of values of n, eventually becoming of order 10^{-7} for the highest values of n for which they have been deduced from data on satellite orbits. The essential point is that both the zonal and the tesseral-sectorial coefficients maintain this order of magnitude out to high values of n, say 15 or 20. For $n=15$ there are 250 coefficients and for $n=20$ there are 435. Moreover, for the zonals the long-periodic effect on a satellite orbit is proportional to $J_n/J_2 = 0(J_2)$, so that this failure of the coefficients to diminish rapidly can be expected to have important effects. These effects would be especially serious if one wants to calculate a satellite orbit accurately enough for use as a base line in satellite geodesy or oceanography. In the latter case one would like to obtain an accuracy of 10 cm. Laser and radar altimeters may well be developed that will furnish instrumental accuracy of such an order. The bottleneck would then be inaccuracy in the calculated orbital base line, arising from lack of knowledge of the Earth's gravitational field. (Of course drag also causes difficulty at present, but drag-free satellites are expected to be developed eventually.) To track satellites, it is sufficient to calculate the orbit from the first few coefficients, with occasional reinitialization. For accurate satellite geodesy, however, a highly improved knowledge of the Earth's field appears desirable.

With the advent of the method of Lie transforms (Deprit and Rom, 1968; Deprit, 1969; Hori, 1966), it may become possible to do both the analytical developments and the numerical calculation for a satellite orbit, in a systematic way with a digital computer, even when many harmonics are included in the potential. The doubt may remain, however, about the accuracy of determination of the coefficients of potential and thus about the resulting accuracy of the orbit.

All in all, it appears desirable to find some method to supplement the spherical harmonic specification of the Earth's potential. The slow falling off of these harmonics, as n increases, furnishes a clue to one possibility, that of a surface layer having a mass density of variable sign. If ϱ is the volume density within the Earth and $d\tau$ a volume element, the normalized coefficients of potential are given by

$$M\bar{C}_{n0} = (2n+1)^{-1/2} \int (r/R)^n\, P_n(\cos\theta)\, \varrho\, d\tau \tag{10}$$

$$M(\bar{C}_{n,m} + i\bar{S}_{n,m}) = \left[\frac{2(n-m)!}{(2n+1)(n+m)!}\right]^{1/2} \int (r/R)^n\, P_n^m(\cos\theta) \times \exp(im\lambda)\, \varrho\, d\tau, \quad (n \geqq 2) \tag{11}$$

where r, θ, and λ are now the geocentric coordinates of a source point.

To obtain some idea of the effect on the potential coefficients of the factors in front of the integrals, consider the limiting cases $m=0$ and $m=n$.

For $m=0$ we have for large n

$$P_n(\cos\theta) \approx \left(\frac{2}{\pi n \sin\theta}\right)^{1/2} \sin\left[(n+\tfrac{1}{2})\,\theta + \frac{\pi}{4}\right]. \tag{11.1}$$

Then (10) and (11.1) give

$$M\bar{C}_{n0} \approx n^{-1}\,\pi^{-1/2} \int (r/R)^n\,(\csc\theta)^{1/2} \sin\left[(n+\tfrac{1}{2})\,\theta + \frac{\pi}{4}\right] \varrho\,\mathrm{d}\tau\,. \tag{11.2}$$

For $m=n$ we have

$$P_n^n(\cos\theta) = \frac{(2n)!}{2^n n!} \sin^n\theta\,, \tag{11.3}$$

so that

$$M(\bar{C}_{n,n} + i\bar{S}_{n,n}) = \left(\frac{2}{2n+1}\right)^{1/2} \frac{[(2n)!]^{1/2}}{2^n n!} \times$$
$$\times \int (r/R^n) \sin^n\theta \exp(im\lambda)\,\varrho\,\mathrm{d}\tau\,, \tag{11.4}$$

by (11) and (11.3). With use of Stirling's formula for large n, this becomes

$$M(\bar{C}_{n,n} + i\bar{S}_{n,n}) \approx \pi^{-1/4}\,n^{-3/4} \int (r/R)^n \sin^n\theta \exp(in\lambda)\,\varrho\,\mathrm{d}\tau\,. \tag{11.5}$$

Thus the factors cannot produce any rapid variation of the C's and S's with increasing n.

Any rapid variation of the C's and S's with increasing n would have to be produced by the factor $(r/R)^n$ in the integrands. The actual slow variation of the coefficients with n is thus rather interesting. If the density anomalies that give rise to the higher harmonics were deep within the Earth, the factor $(r/R)^n$ would lead to a rapid diminution of the coefficients with increasing n. Since, however, the coefficients fall off very slowly as n increases, it follows that the higher harmonics must arise from density anomalies close to the surface of the Earth. They have, therefore, nothing to do with the approximately ellipsoidal shape of the Earth, which is related to the large J_2. There is thus no reason to suppose that the coefficients would fall off faster, with increasing order, if the expansion were written in terms of spheroidal or general ellipsoidal harmonics, instead of spherical harmonics.

There is an expression for the Earth's potential in spheroidal coordinates (Vinti, 1966), which is accurate everywhere to a few parts in a million and which leads to an integrable problem for a purely gravitational orbit, but the accuracy of this potential depends on a fit to μ, J_2, and J_3 only. Those few parts in a million which are thereby lost, although of little practical importance in tracking, are just the parts that are so

important for satellite geodesy and they are presumably not related to the main departure from spherical shape.

We are thus led naturally to the following attempt. Write the Earth's potential as

$$V = V_p + \delta V\,. \tag{12}$$

Here V_p is to be either a sum of the first few terms in the spherical harmonic expansion or the spheroidal potential (Vinti, 1966). The correction δV is to be expressed by means of a surface layer of variable density and variable sign, distributed over a sphere just including the Earth.

2. The Effective Surface Layer

Suppose that V_p denotes the spherical harmonic expansion, through harmonics of order p, whose coefficients may be assumed to be accurately known. Then

$$\delta V = -\,G \int_S \frac{\sigma(\theta', \lambda)\,\mathrm{d}S'}{|\mathbf{r} - \mathbf{r}'|}\,. \tag{13}$$

Here S is a sphere of radius a that just clears the Earth, with center at the center of mass of the Earth, $\mathbf{r}$ is the position vector of a field point, $\mathbf{r}'$ is that of a source point on the spherical surface, $\mathrm{d}S' = a^2 \sin\theta'\,\mathrm{d}\theta'\,\mathrm{d}\lambda'$, and $\sigma(\theta', \lambda')$ is a fictitious surface density of mass on S. The necessary σ is

$$\sigma(\theta', \lambda') = \frac{M}{2\pi a^2} \sum_{n=p+1}^{\infty} (n + \tfrac{1}{2}) \left(\frac{R}{a}\right)^n \Bigg[- J_n P_n(\cos\theta') + \sum_{m=1}^{n} P_n^m(\cos\theta')\,(C_{n,m} \cos m\lambda' + S_{n,m} \sin m\lambda') \Bigg]. \tag{14}$$

Then Equations (12), (13), and (14) are together equivalent to Equation (1). To show this, expand $|\mathbf{r} - \mathbf{r}'|^{-1}$ as a generating function of a series in $P_k(\cos\psi)$, where ψ is the angle between $\mathbf{r}$ and $\mathbf{r}'$, use the addition theorem for spherical harmonics, insert these results into (13) and (14), and perform the integration, with use of the various orthogonality properties. The resulting surface density σ has the property that the appropriate surface integrals of it over the sphere, obtained from (10) and (11) by replacing r by a and $\varrho\,\mathrm{d}\tau$ by $\sigma\,\mathrm{d}S$, give zero contributions to M and to all the coefficients of potential through J_p, $C_{p,p}$, and $S_{p,p}$.

Although Equation (14) is for a surface layer on a sphere clearing the Earth, if we take $a = R$ it should represent, at least approximately, the variations in Earth density near the surface of the Earth. Suppose we know σ at a point on the Earth. If we then take the thickness of the anomalous region to be that of the Earth's crust, viz. b, then $\sigma/b = \Delta\varrho$, the anomaly in the volume density in that region. With some knowledge of the crustal thickness, we can thus find out if σ has a reasonable value.

3. Relation of the Effective Surface Layer to Gravity Measurements

From (1)

$$\delta V = -\frac{\mu}{r}\sum_{n=p+1}^{\infty}\left(\frac{R}{r}\right)^n F_n, \tag{15}$$

where

$$F_n \equiv -J_n P_n(\cos\theta) + \sum_{m=1}^{n} P_n^m(\cos\theta)\,(C_{n,m}\cos m\lambda + S_{n,m}\sin m\lambda). \tag{16}$$

Then

$$2\frac{\partial\delta V}{\partial r} + \frac{\delta V}{r} = \frac{\mu}{r^2}\sum_{n=p+1}^{\infty}(2n+1)\left(\frac{R}{r}\right)^n F_n \tag{17}$$

and on the sphere of radius a

$$2\left(\frac{\partial\delta V}{\partial r}\right)_a + \frac{(\delta V)_a}{a} = \frac{\mu}{a^2}\sum_{n=p+1}^{\infty}(2n+1)\left(\frac{R}{a}\right)^n F_n. \tag{18}$$

Comparison of (14), (16), and (18) then shows that

$$4\pi G\sigma = 2\left(\frac{\partial\delta V}{\partial r}\right)_a + \frac{(\delta V)_a}{a}. \tag{19}$$

Now the geopotential Ω is given by

$$\Omega = V - \tfrac{1}{2}\omega^2 r^2\sin^2\theta, \tag{20}$$

where ω is the Earth's sidereal rate of rotation. The acceleration of gravity $\mathbf{g}$ is then given by

$$\mathbf{g} = \nabla\Omega, \tag{21}$$

so that its radial component g_r (taken positive toward the Earth) is

$$g_r = \frac{\partial\Omega}{\partial r} = \frac{\partial V}{\partial r} - \omega^2 r\sin^2\theta. \tag{22}$$

Thus

$$\frac{\partial\delta V}{\partial r} = g_r + \omega^2 r\sin^2\theta - \frac{\partial V_p}{\partial r}, \tag{23}$$

by (22) and (12). Then, by (19) and (23),

$$4\pi G\sigma = 2\left[(g_r)_a + \omega^2 a\sin^2\theta - \left(\frac{\partial V_p}{\partial r}\right)_a\right] + \frac{(V - V_p)_a}{a}. \tag{24}$$

In (24) the unknowns are $(g_r)_a$ and V_a. Some simple estimates show that the second term, $(V-V_p)_a/a$, does not amount to more than about 10% of the first.

If a world-wide accurate gravity survey were available, we should know g_r at sufficiently many points on the Earth. The problem in finding σ from such gravity data would then be mainly to find a method of extending g_r from the Earth to its value $(g_r)_a$ on the surface of the sphere of radius a. To find $(V-V_p)_a/a$ we should also need to know V_a. Over the oceans this problem would be solvable once the extension of g_r is known. To see this, note that by (21)

$$\Omega_a(\theta, \lambda) - \Omega_e = \int_{\mathbf{r}_G}^{\mathbf{a}} \mathbf{g}\cdot d\mathbf{r} = \int_{r_G}^{a} g_r \, dr, \tag{25}$$

where Ω_e is the constant geopotential of the oceans and r_G is the radius of the geoid (mean ocean surface) at geocentric colatitude θ and longitude λ. Then, by (20) and (25),

$$V_a(\theta, \lambda) = \Omega_e + \tfrac{1}{2}\omega^2 a^2 \sin^2\theta + \int_{r_G}^{a} g_r \, dr. \tag{26}$$

Over the land the problem would not be so simple, since the geoid there is usually below the surface.

Since such a gravity survey is not yet available, it is possible at this time only to use coefficients of potential, mostly determined from satellite orbits, to test the general validity of the surface-layer concept. Before we do this, however, it is of interest to consider the relation of Legendre and inverse Legendre transforms to the present problem.

4. Legendre Transforms

If a function $f(\xi)$ is expandable as a converging series of Legendre polynomials, of the form

$$f(\xi) = \sum_{n=0}^{\infty} (n + \tfrac{1}{2}) f_n P_n(\xi), \quad (-1 \leqq \xi \leqq 1) \tag{26.1}$$

then

$$f_n = \int_{-1}^{1} f(\xi) P_n(\xi) \, d\xi \tag{27}$$

and the set of coefficients $\{f_n\}$ is called the Legendre transform of $f(\xi)$.

Now suppose we neglect departures of σ from axial symmetry. It would then satisfy the equation

$$\sigma(\cos\theta) = \sum_{n=0}^{\infty} (n + \tfrac{1}{2}) f_n P_n(\cos\theta), \tag{28}$$

where

$$f_n = 0 \quad (0 \leqq n \leqq p) \tag{28.1}$$

$$f_n = -\frac{M}{2\pi a^2}\left(\frac{R}{a}\right)^n J_n \quad (n \geqq p+1). \tag{28.2}$$

For simplicity, we may consider the case where $a=R$, thus neglecting the part of Mount Everest which juts out beyond the equatorial radius. For $n>p$ and except for a constant factor, the J's are then the Legendre transform of the layer density σ and, conversely, σ is the inverse Legendre transform of the J's (and the vanishing f_n's). Inspection of a table of Legendre transforms (Churchill, 1954) shows that if the J's behave asymptotically like n^{-1}, σ has a term like $(1\text{-}\cos\theta)^{-1/2}$, with a singularity at the north pole. If the behavior is like $(-1)^n n^{-1}$, σ contains a term like $(1+\cos\theta)^{-1/2}$, with a singularity at the south pole. If the behavior is like n^{-2}, σ has a logarithmic term, again with a singularity at one of the poles. It would take a somewhat more complicated form for $J_n(n)$ to produce a singularity in σ at any other latitude.

If the J's fell off faster than n^{-2}, the series for σ would converge absolutely for all θ, so that σ would not have any singularities. (Note that any singularity in σ corresponding to a point mass on the sphere would still permit convergence of the series for the potential.) Examination of Kozai's table for the J's (Kozai, 1967, p. 52) gives no indication that they fall off faster than n^{-2}. Apparently the situation is just on the edge of permitting singularities, so that the behavior of the coefficients is compatible with the existence of quasi-singularities or mass concentrations. The existence of such mass concentrations (mascons) is thus not surprising. If the coefficients fell off appreciably faster than n^{-2}, however, one would not expect to find them. Shortly after such mascons were discovered on the Moon, Kaula (1969) and others began finding similar concentrations on the Earth. To sum up: the behavior of the coefficients is such as would be expected if mascons exist.

Churchill's table of Legendre transforms can be extended by means of a convolution theorem (Churchill and Dolph, 1954). One form of this states that if $\{f_n\}$ and $\{g_n\}$ are the respective Legendre transforms of $f(\cos\theta)$ and $g(\cos\theta)$, then the inverse Legendre transform of $\{f_n g_n\}$, viz $h(\cos\theta)$, is given by

$$h(\cos\theta) = (2\pi)^{-1} \int_S f(\cos\alpha)\, g(\cos\beta)\, \mathrm{d}S\,, \tag{29}$$

where S is a unit sphere. In evaluating this integral θ is to be thought of as a fixed side of a spherical triangle and α and β as variable sides, intersecting in a point P at the surface element $\mathrm{d}S$.

In the general case of axial asymmetry, the set of coefficients J_n, $C_{n,m}$ and $S_{n,m}$ $(n>p)$, plus the zero values for $n\leqq p$, may be termed the spherical harmonic transform of σ (except for a constant factor, see Equation (14)). For a better understanding of the relations connecting the surface layer and the spherical harmonic transform, it would be desirable to have a corresponding generalized convolution theorem. Unfortunately no such theorem is yet known.

There is, however, an enormous literature on spherical harmonics, as well as a developing fund of information on Legendre and inverse Legendre transforms. It is thus likely that the corrections to the Earth's potential may be more conveniently represented by a surface layer on a sphere than by such a layer on the Earth itself, on

the geoid, or on an ellipsoid. This conjecture is strengthened by the physical remark that the density anomalies that give rise to the higher terms in the potential have little or nothing to do with the J_2 that is a result of the Earth's approximately ellipsoidal shape.

5. Recursion Formulas

To test the idea of a surface layer, it is desirable to construct some contour maps of σ from those values that are known for the coefficients of potential. In doing so, one needs to compute $P_n(\cos\theta)$ and $P_n^m(\cos\theta)$ out to high values of n and m. Now $P_n(\xi)$ is a polynomial with alternating signs and so is

$$P_n^{(m)}(\xi) \equiv \mathrm{d}^m P_n(\xi)/\mathrm{d}\xi^m, \tag{30}$$

where

$$P_n^m(\xi) \equiv (1-\xi^2)^{m/2}\, P_n^{(m)}(\xi). \tag{31}$$

One may avoid the loss of accuracy that would arise from the alternations in sign by building up the polynomials recursively.

To do so, one may use the following well known formula for the P_n's:

$$nP_n(\xi) \equiv (2n-1)\,\xi P_{n-1}(\xi) - (n-1)\,P_{n-2}(\xi) \tag{32}$$

and an easily derived formula for the sectorials:

$$P_n^n(\xi) \equiv (2n-1)\,(1-\xi^2)^{1/2}\, P_{n-1}^{n-1}(\xi). \tag{33}$$

For the tesserals one may use

$$(n-m+1)\,P_{n+1}^m(\xi) \equiv (2n+1)\,\xi P_n^m(\xi) - (n+m)\,P_{n-1}^m(\xi) \tag{34}$$

and

$$P_n^m(\xi) \equiv 2(m-1)\,\xi\,(1-\xi^2)^{-1/2}\, P_n^{m-1}(\xi) - \\ -(n-m+2)\,(n+m-1)\,P_n^{m-2}(\xi), \tag{35}$$

derived by my assistant Dr R. H. Djojodihardjo.

With use of Equations (8) these recursion formulas can all be written in terms of the normalized polynomials or functions.

6. Use of the Spheroidal Potential

Instead of taking δV to be $V - V_p$, as above defined, I took

$$\delta V = V - V_0. \tag{36}$$

Here V_0 is the spheroidal potential (Vinti, 1966), given by

$$V_0 = -\mu \frac{\varrho + \eta\delta}{\varrho^2 + c^2\eta^2}, \tag{37}$$

where ϱ and η are spheroidal coordinates and where

$$c^2 = c_0^2 - \delta^2 \tag{38.1}$$

$$c_0^2 = R^2 J_2 \tag{38.2}$$

$$\delta = \tfrac{1}{2} R\,|J_3|\,J_2^{-1}\,. \tag{38.3}$$

Its expansion in spherical harmonics is given by

$$V_0 = -\frac{\mu}{r}\left[1 - \left(\frac{R}{r}\right)^2 J_2 P_2(\cos\theta) - \left(\frac{R}{r}\right)^3 J_3 P_3(\cos\theta) - \right.$$
$$\left. - \left(\frac{R}{r}\right)^4 J_4^* P_4(\cos\theta) + 0(J_2^3)\right], \tag{39}$$

where

$$J_4^* = -J_2^2 + J_3^2/J_2\,, \tag{39.1}$$

with the same sign as J_4 and about two-thirds of its numerical value. Higher terms are essentially negligible in the expansion of (37).

Then Equation (14) for σ gets changed to

$$\sigma(\theta, \lambda) = \frac{M}{4\pi a^2} - \left[9\left(\frac{R}{a}\right)^4 (J_4 - J_4^*)\, P_4(\cos\theta) - \right.$$
$$- \sum_{n=5}^{\infty} (2n+1)\left(\frac{R}{a}\right)^n J_n P_n(\cos\theta) +$$
$$+ \sum_{n=2}^{\infty} (2n+1)\left(\frac{R}{a}\right)^n \sum_{m=1}^{n} P_n^m(\cos\theta) \times$$
$$\left. \times (C_{n,m}\cos m\lambda + S_{n,m}\sin m\lambda)\right]. \tag{40}$$

In practice, to see how things were going, I took $a = R$ and used an upper limit $n = N$, corresponding to the availability of data. Then

$$G\sigma = \frac{\mu}{4\pi R^2}\left[-9(J_4 - J_4^*)\, P_4(\cos\theta) - \sum_{n=5}^{N} (2n+1)\, J_n P_n(\cos\theta) + \right.$$
$$\left. + \sum_{n=2}^{N} (2n+1) \sum_{m=1}^{n} P_n^m(\cos\theta)\,(C_{n,m}\cos m\lambda + S_{n,m}\sin m\lambda)\right] \tag{41}$$

where $C_{2,1} = S_{2,1} = 0$. The resulting σ, as computed by (41), is then the surface density of a spherical layer whose potential represents the difference between the spheroidal potential and the Earth's actual potential, as currently known.

7. Computations and Contour Maps

Values of the coefficients were obtained from two sources, Rapp and Köhnlein (both

1967) and Kozai (1967) (the latter being abbreviated to SAO). These coefficients correspond to the following values of μ and R.

	Rapp	SAO
μ	(3.986009) 10^4 m^3/s^2	same
R	6378138 m	6378142 m

Kozai's values for the zonal coefficients were derived from Baker-Nunn observations of artificial satellites, with orbital inclinations ranging from 28° to 96°. Köhnlein's values for the non-zonal coefficients came from a combination of satellite data and gravity anomalies, as did Rapp's data for all the coefficients.

In building up the polynomials P_n and the functions P_n^m from the recursion formulas (32) through (35) it was found convenient, for practical numerical reasons, to calculate the normalized values by combining (32) through (35) with the normalization rules given in Equations (8).

To compare the values of σ resulting from the two sets of data, it was desirable to use the same V_0 for both. Since the μ's are equal and the R's almost so, this requirement amounts in practice to using mean values J_2^*, J_3^*, and J_4^{**} in V_0. Here

$$2J_2^* = J_2\,(\text{Rapp}) + J_2\,(\text{SAO}) \tag{42.1}$$

$$2J_3^* = J_3\,(\text{Rapp}) + J_3\,(\text{SAO}) \tag{42.2}$$

$$J_4^{**} = -J_2^{*2} + J_3^{*2}/J_2^*. \tag{42.3}$$

This procedure results in a slight change in Equation (41), which then becomes.

$$G\sigma = \frac{\mu}{4\pi R^2}\Bigg[-5\,(J_2 - J_2^*)\,P_2\,(\cos\theta) - 7\,(J_3 - J_3^*)\,P_3\,(\cos\theta) - \\ - 9\,(J_4 - J_4^{**})\,P_4\,(\cos\theta) - \sum_{n=5}^{N}(2n+1)\,J_n P_n\,(\cos\theta) + \\ + \sum_{n=2}^{N}(2n+1)\sum_{m=1}^{n} P_n^m\,(\cos\theta)\,(C_{n,m}\cos m\lambda + S_{n,m}\sin m\lambda)\Bigg]. \tag{43}$$

As noted before, the actual computing program for (43) had to be written with normalized P's and coefficients.

After calculation, the values of $G\,\sigma$ were converted by a CalComp digital plotter into contour maps of $G\,\sigma$ versus θ and λ. The first result noted was that the number of extrema of σ increased as N was increased. Thus with $N=8$, Rapp's data gave 11 minima and 10 maxima; with $N=14$ his data gave 45 extrema.

Appendix A gives values of $G\,\sigma$ obtained from (43) with $N=14$. Table I is for the SAO data and Table II for Rapp's data. The values of θ run from 0° to 180°, at intervals of 10°. Those for the longitude λ (denoted by 'PHI' in the tables) range from −175° to 180°, at intervals of 5°. The numerical values are for $10^6\,G\sigma$ in units of m/s^2. The rms values of $10^6\,G\sigma$ are 16.7 m/s^2 for the Rapp data and 16.8 m/s^2 for the SAO data.

Appendix B gives contour maps of $10^6\,G\sigma$, again in units of m/s^2. The maps obtained from the two sets of data agree at least qualitatively and in some places quite

well. The complexity of the maps and the large number of extrema, however, make it apparent that the original plan for curve-fitting a simple formula for σ, as a function of θ and λ, cannot be achieved.

If we let

$$10^6\, G\sigma\,(\text{in m/s}^2) \equiv Q\,, \tag{44}$$

then since $G=(6.66)\ 10^{-8}$ cgs units, we have

$$\sigma = 1500\, Q\ \text{g/cm}^2\,. \tag{45}$$

With a rms value $Q=17$, we find

$$\sigma\,(\text{rms}) = 25\,500\ \text{g/cm}^2\,. \tag{46}$$

Suppose we now assume that the density anomalies that give rise to the higher coefficients of potential all occur in the crust, of thickness b. The fluctuation $\Delta\varrho$ in the volume density ϱ, corresponding to a given σ, is

$$\Delta\varrho = \sigma/b\,. \tag{47}$$

With a mean value $b=30$ km (Heiskanen and Moritz, 1967), we then find

$$\Delta\varrho\,(\text{rms}) = \frac{25\,500}{(3)\ 10^6} = 0.0085\ \text{g/cm}^3\,. \tag{48}$$

Inspection of the tables and the maps shows that ± 100 are plausible bounds for Q. With $b=30$ km, (47) then gives

$$|\Delta\varrho|_{\max} = 0.05\ \text{g/cm}^3\,. \tag{49}$$

Even if we allow for a much thinner crust in certain regions, say 10 km on the ocean bottom, $|\Delta\varrho|$ would still not exceed 0.15 g/cm^3. These are reasonable results.

8. Conclusions

The contour maps, along with the numerical values of σ, show that the concept of a surface layer is, at least in principle, a feasible method of representing the departures of the Earth's gravitational potential from a reference potential.

Acknowledgements

Dr R. H. Djodjodihardjo developed the recursion formulas for the associated Legendre polynomials and programmed and carried out the numerical computations, with the aid of Mr Carl Goodwin. Dr S. J. Madden took part in many useful discussions and contributed valuable suggestions about the computation.

References

Churchill, R. V.: 1954, *J. Math. Phys.* **33**, 165–178.
Churchill, R. V. and Dolph, C. L.: 1954, *Proc. Am. Math. Soc.* **5**, 93–100.
Deprit, A.: 1969, *Celes. Mech.* **1**, 12–30.

Deprit, A. and Rom, A.: 1968, *The Main Problem of Satellite Theory for Small Eccentricities*, Boeing Scientific Research Laboratories, Mathematical Note No. 615, D1-82-0888.
Heiskanen, W. and Moritz, H.: 1967, *Physical Geodesy*, W. H. Freeman and Company, San Francisco and London, p 136.
Hori, G.: 1966, *Publ. Astron. Soc. Japan* **18**, 287–96.
Kaula, W.: 1969, Lecture at the Summer Institute in Dynamical Astronomy, MIT.
Köhnlein, W.: 1967, Smithsonian Astrophysical Observatory Special Report 264, pp. 57–72.
Kozai, Y.: 1967, Smithsonian Astrophysical Observatory Special Report 264, pp. 43–56.
Rapp, R. H.: 1967, 'The Geopotential to (14, 14) from a Combination of Satellite and Gravimetric Data', paper presented at the XIV General Assembly, IUGG-IAG, Fall 1967, Lucerne, Switzerland.
Rapp, R. H.: 1968, *J. Geophys. Res.* **73**, 6555–62.
Vinti, J. P.: 1966, *J. Res. Nat. Bur. of Std.* **70B**, 1–16, 17–46.

Appendix A

TABLE I

Distribution of surface density $10^6\ G\sigma$ in m/sec^2 (SAO)

Theta	180	170	160	150	140	130	120	110	100	90	80	70	60	50	40	30	20	10	0
Phi																			
—175.0 Deg	—1.0	—41.2	—58.3	—44.4	— 8.3	7.5	19.7	36.0	9.5	—10.0	1.6	— 2.4	—10.0	—15.0	— 5.2	9.8	—12.4	— 8.4	16.5
—170.0 Deg	—1.0	—43.8	—60.8	—47.8	—16.7	5.3	10.4	18.4	9.9	— 9.7	— 1.0	5.1	— 4.1	—16.8	—12.8	6.2	—12.0	— 9.0	16.6
—165.0 Deg	—1.0	—45.8	—61.8	—49.0	—24.0	3.1	0.3	0.3	15.9	0.2	3.1	14.4	— 0.5	—17.0	—13.8	7.8	— 9.6	— 9.2	16.6
—160.0 Deg	—1.0	—47.1	—61.0	—47.2	—29.0	4.2	— 1.1	— 8.8	22.3	12.3	14.1	25.4	0.5	—15.9	— 8.9	13.5	— 5.8	— 8.9	16.6
—155.0 Deg	—1.0	—47.8	—58.7	—42.2	—29.0	7.7	7.1	— 5.7	26.2	19.2	25.2	33.9	— 0.7	—14.3	— 1.8	20.9	— 1.4	— 8.3	16.6
—150.0 Deg	—1.0	—47.8	—55.1	—34.7	—25.1	7.9	13.8	1.2	25.5	17.8	27.2	33.1	— 4.1	—13.9	2.7	26.7	2.7	— 7.4	16.6
—145.0 Deg	—1.0	—47.2	—50.6	—26.0	—21.6	— 0.3	6.0	— 1.7	18.7	10.3	16.6	20.0	—10.0	—16.4	1.0	28.1	5.5	— 6.3	16.6
—140.0 Deg	—1.0	—45.9	—45.4	—17.5	—18.5	—15.4	—16.8	—17.4	7.4	2.1	— 0.6	— 0.4	—17.8	—22.5	— 7.0	24.2	6.3	— 5.1	16.6
—135.0 Deg	—1.0	—44.0	—39.9	—10.3	—15.7	—29.3	—38.7	—33.8	— 2.2	— 2.8	— 2.2	—18.5	—26.1	—30.5	—18.0	15.7	4.9	— 3.9	16.6
—130.0 Deg	—1.0	—41.7	—34.3	— 5.0	—33.6	—33.6	—45.8	—34.9	— 4.0	— 4.6	—20.0	—27.9	—33.3	—36.2	—26.2	4.8	1.5	— 2.7	16.6
—125.0 Deg	—1.0	—38.8	—28.7	— 1.6	— 9.2	—26.8	—32.5	—18.9	1.6	— 7.0	—20.0	—29.0	— 38.6	—35.4	—26.6	— 6.0	— 3.6	— 1.5	16.6
—120.0 Deg	—1.0	—35.6	—23.1	0.4	— 6.2	—15.6	—14.2	— 0.9	7.4	—12.3	—19.8	—26.4	—40.9	—25.8	—17.5	—15.0	— 9.5	— 0.4	16.6
—115.0 Deg	—1.0	—32.2	—17.4	1.7	— 4.4	— 8.2	— 7.8	— 2.1	7.5	—18.4	—21.5	—23.1	—39.0	— 9.3	— 2.3	—21.9	—15.6	0.6	16.6
—110.0 Deg	—1.0	—28.6	—11.9	3.0	— 3.4	— 6.6	—15.8	—10.8	3.2	—21.0	3.2	—21.0	—32.6	8.0	12.2	—27.5	—21.1	1.7	16.6
—105.0 Deg	—1.0	—24.9	— 6.4	4.5	— 2.1	— 6.5	—25.3	—23.6	1.1	—17.9	—20.5	—10.4	—22.6	19.7	18.7	—33.0	—25.6	2.7	16.6
—100.0 Deg	—1.0	—21.2	— 1.4	6.0	0.1	— 2.7	—22.6	—21.7	5.0	—11.3	—13.0	1.9	—11.9	10.0	13.5	—39.1	—28.7	3.8	16.6
— 95.0 Deg	—1.0	—17.6	3.1	7.2	2.6	4.6	8.4	— 7.3	10.0	— 4.4	— 0.9	15.5	— 4.0	6.8	— 1.7	—45.0	—30.2	5.0	16.6
— 90.0 Deg	—1.0	—14.2	7.0	7.4	3.8	10.0	3.7	3.8	8.8	1.2	13.7	25.0	— 1.2	— 8.8	—20.5	—49.4	—29.9	6.3	16.6
— 85.0 Deg	—1.0	—11.0	10.1	6.6	2.7	8.9	2.7	1.6	0.9	7.0	17.2	24.7	— 4.7	—21.4	—35.3	—50.5	—28.0	7.7	16.6
— 80.0 Deg	—1.0	— 8.1	12.5	5.2	— 0.1	3.4	— 7.2	— 6.0	— 3.7	1.52	34.9	11.9	—14.1	—26.8	—41.4	—47.6	—24.8	9.1	16.6
— 75.0 Deg	—1.0	— 5.5	1.44	4.1	— 2.4	0.0	—11.0	— 1 1	5.6	25.4	33.7	—10.8	—27.6	—25.5	—38.6	—41.1	—20.7	10.6	16.6
— 70.0 Deg	—1.0	— 3.3	16.0	4.3	— 2.3	3.4	0.0	22.0	27.5	33.0	23.5	—36.0	—41.5	—22.1	—30.8	—32.4	—16.4	12.1	16.6
— 65.0 Deg	—1.0	— 1.4	17.5	6.6	0.1	11.0	18.1	47.9	46.6	31.3	6.2	—55.2	—51.0	—20.2	—22.7	—23.4	—11.2	13.5	16.6
— 60.0 Deg	—1.0	0.3	18.8	11.1	3.5	15.3	25.9	53.1	45.9	16.5	—15.2	—63.2	—51.4	—20.2	—16.9	—15.2	— 6.4	15.0	16.6
— 55.0 Deg	—1.0	1.6	20.0	16.9	5.9	11.0	14.5	29.9	23.8	— 7.0	—36.9	—59.7	—40.4	—18.4	—12.4	— 7.9	— 1.6	16.5	16.6
— 50.0 Deg	—1.0	2.7	20.7	23.0	6.3	0.0	— 7.7	— 5.7	— 4.3	—27.6	—52.6	—48.1	—20.5	—10.7	— 6.2	— 0.8	3.3	17.9	16.6
— 45.0 Deg	—1.0	3.6	20.9	28.2	5.4	—10.8	—23.1	—29.4	—20.6	—34.5	—55.8	—33.1	1.7	4.2	4.4	7.0	8.7	19.2	16.6
— 40.0 Deg	—1.0	4.3	20.2	31.7	4.0	—16.0	—22.6	—31.3	—20.5	—26.2	—44.8	—19.6	18.3	23.4	19.3	16.0	14.5	20.5	16.6
— 35.0 Deg	—1.0	4.9	18.6	37.8	1.5	—16.1	—12.2	—14.8	—11.5	—24.6	—10.9	24.5	40.9	35.1	35.1	25.7	20.7	21.6	16.6

TABLE I *(continued)*

Distribution of surface density $10^6\ G\sigma$ in m/s² (SAO)

Theta	180	170	160	150	140	130	120	110	100	90	80	70	60	50	40	30	20	10	0
Phi																			
— 30.0 Deg	—1.0	5.5	16.3	31.9	1.0	—15.7	— 5.6	—17.1	—14.7	— 0.5	— 3.7	— 6.7	21.7	51.6	47.0	34.7	27.1	22.5	16.6
— 25.0 Deg	—1.0	6.2	13.3	29.4	— 0.2	—18.1	— 9.2	—21.0	—19.7	4.4	13.1	— 2.7	16.6	54.0	51.1	41.6	33.4	23.2	16.6
— 20.0 Deg	—1.0	7.1	10.1	26.4	— 0.4	—21.9	—16.7	—24.0	—21.2	7.2	26.3	5.6	16.3	5.02	46.7	45.5	38.8	23.5	16.6
— 15.0 Deg	—1.0	7.9	6.1	23.7	1.2	—23.0	—16.7	—16.5	—15.4	11.1	36.7	17.2	22.4	44.3	36.6	46.4	43.1	23.5	16.6
10.0 Deg	—1.0	9.0	4.6	21.9	5.0	—19.1	— 7.9	— 0.7	— 8.2	13.9	42.5	25.8	31.2	40.6	25.9	45.1	45.6	23.1	16.6
— 5.0 Deg	—1.0	10.4	2.8	20.9	10.2	—11.4	6.8	13.2	— 6.7	13.5	41.2	25.8	37.5	41.1	19.0	42.7	46.2	11.3	16.6
0.0 Deg	—1.0	12.0	1.8	20.4	15.3	— 3.6	18.1	18.1	— 9.7	12.5	35.4	19.1	39.1	45.0	18.1	39.8	44.6	21.0	16.6
5.0 Deg	—1.0	13.8	1.7	19.9	19.2	2.2	22.6	16.5	— 9.1	15.2	31.1	14.3	37.0	48.9	21.8	36.7	41.6	19.4	16.6
10.0 Deg	—1.0	15.9	2.3	19.1	21.7	6.7	23.1	14.7	— 2.1	19.3	30.4	17.1	31.7	48.2	26.7	33.1	36.9	17.4	16.6
15.0 Deg	—1.0	18.1	3.8	17.9	23.1	11.4	23.8	14.4	3.9	16.0	29.0	24.2	21.9	40.4	29.4	28.7	31.3	15.2	16.6
20.0 Deg	—1.0	20.4	5.8	16.8	24.3	16.5	24.8	12.7	1.2	1.3	21.3	27.2	7.7	27.7	28.7	23.7	25.1	12.8	16.6
25.0 Deg	—1.0	22.7	8.5	16.3	25.7	19.7	23.0	7.8	— 7.7	—16.1	9.9	22.2	— 5.6	17.2	25.7	18.6	19.3	10.4	16.6
30.0 Deg	—1.0	25.0	11.7	16.8	27.5	18.9	15.8	2.0	—12.5	—21.7	3.4	14.0	— 9.6	15.9	22.6	14.5	14.4	8.1	16.6
35.0 Deg	—1.0	27.2	15.3	18.7	30.1	14.3	4.6	— 1.0	— 8.7	—12.2	6.0	9.1	0.2	24.7	20.1	12.1	10.7	5.9	16.6
40.0 Deg	—1.0	29.1	19.0	21.9	33.8	9.4	— 5.6	— 1.1	— 4.4	— 1.0	11.4	7.8	17.6	36.9	16.9	11.4	8.2	3.9	16.6
45.0 Deg	—1.0	30.8	22.8	25.7	38.8	8.5	— 9.7	— 0.8	—10.6	— 4.5	8.5	3.8	30.1	41.4	10.7	12.0	6.5	2.1	16.6
50.0 Deg	—1.0	32.2	26.2	29.3	44.2	13.7	— 5.8	— 1.3	—27.0	—23.7	— 5.4	— 6.4	28.6	31.7	0.3	12.8	5.3	0.5	16.6
55.0 Deg	—1.0	33.1	29.1	32.0	48.5	23.0	2.8	— 1.0	—40.8	—44.1	—22.4	—18.3	16.1	10.7	—13.0	12.7	3.7	— 0.7	16.6
60.0 Deg	—1.0	33.6	31.2	33.1	50.1	32.0	10.8	1.2	—40.6	—52.8	—33.6	—23.5	3.9	—11.5	—25.6	10.6	1.3	— 1.7	16.6
65.0 Deg	—1.0	33.7	32.4	32.5	48.3	37.2	13.9	3.3	—29.6	—51.8	—39.2	—20.2	— 0.4	—25.4	—34.3	5.8	— 2.4	— 2.5	16.6
70.0 Deg	—1.0	33.3	32.7	30.5	43.8	37.8	11.9	1.7	—21.8	—54.4	—45.8	—15.7	0.6	—28.7	—38.0	— 1.8	— 7.4	— 2.9	16.6
75.0 Deg	—1.0	32.4	32.0	27.6	37.7	35.4	7.9	— 5.1	—27.6	—67.5	—56.5	—19.0	— 2.6	—26.1	—38.2	—12.0	—13.5	— 3.1	16.6
80.0 Deg	—1.0	31.1	30.5	24.1	30.9	30.6	2.8	—15.1	—44.6	—83.9	—65.1	—30.1	—14.8	—23.9	—37.4	—23.7	—20.0	— 3.1	16.6
85.0 Deg	—1.0	29.5	28.3	20.2	23.2	22.5	— 2.1	—25.7	—60.5	—90.2	—64.0	—42.0	—30.9	—24.6	—36.7	—35.6	—26.3	— 2.7	16.6
90.0 Deg	—1.0	27.5	25.6	15.9	13.9	9.0	—13.4	—35.2	—64.0	—78.8	—52.8	—45.3	—40.4	—26.8	—39.3	—46.0	—31.3	— 2.1	16.6
95.0 Deg	—1.0	25.1	22.6	11.2	2.9	— 9.8	—30.5	—42.6	—51.1	—52.4	—38.9	—40.0	—38.0	—28.4	—41.4	—53.3	—34.6	— 1.3	16.6
100.0 Deg	—1.0	22.6	19.5	6.4	— 8.9	—30.0	—48.3	—45.8	—25.9	—17.9	—27.8	—31.7	—28.5	—29.8	—42.8	—56.3	—35.6	— 0.2	16.6
105.0 Deg	—1.0	19.8	16.4	2.1	—19.3	—45.8	—58.7	—43.4	1.6	17.3	—17.1	—24.8	—20.7	—32.5	—42.3	—55.0	—34.3	0.9	16.6
110.0 Deg	—1.0	16.8	13.5	— 1.3	—26.1	—53.3	—57.4	—35.7	20.1	45.7	— 0.6	—17.1	—18.7	—38.9	—38.9	—49.9	—31.1	2.2	16.6
115.0 Deg	—1.0	13.6	10.8	— 3.4	—28.5	—53.1	—47.5	—25.8	23.8	60.8	23.0	— 3.9	—17.5	—34.5	—31.7	—42.1	—26.3	3.3	16.6
120.0 Deg	—1.0	10.3	8.2	— 4.1	—27.0	—49.7	—37.2	—15.8	18.0	61.7	46.6	15.0	— 9.8	—24.5	—20.8	—32.8	—20.7	4.4	16.6
125.0 Deg	—1.0	6.8	5.6	— 4.0	—22.8	—46.8	—33.0	— 5.8	15.3	55.4	60.8	32.6	6.1	— 5.2	— 7.5	—23.1	—14.9	5.1	16.6
130.0 Deg	—1.0	3.1	2.6	— 3.8	—17.2	—44.6	—34.5	4.6	23.7	51.3	61.7	40.5	24.0	17.3	5.5	—13.6	— 8.4	5.5	16.6

TABLE I *(continued)*

Distribution of surface density $10^6\ G\sigma$ in m/s² (SAO)

Theta	180	170	160	150	140	130	120	110	100	90	80	70	60	50	40	30	20	10	0
Phi																			
135.0 Deg	—1.0	— 0.7	— 0.0	— 4.1	—11.0	—39.7	—25.3	13.9	38.0	51.8	53.3	36.9	35.2	33.8	15.6	— 4.4	— 4.5	5.5	16.6
140.0 Deg	—1.0	— 4.8	— 5.2	— 5.4	— 4.5	—28.9	—28.4	20.2	45.7	51.7	43.4	28.5	36.0	38.1	21.7	4.9	— 0.7	5.1	16.6
145.0 Deg	—1.0	— 9.0	—10.2	— 7.9	1.4	—13.3	—12.5	24.5	41.4	46.0	37.2	24.0	29.5	30.7	24.8	14.1	1.9	4.2	16.6
150.0 Deg	—1.0	—13.3	—16.0	—11.5	5.7	1.9	6.6	30.4	33.6	37.8	34.8	25.5	20.8	17.1	26.9	23.2	3.2	2.9	16.6
155.0 Deg	—1.0	—17.7	—22.5	—15.8	8.0	10.7	20.0	40.0	34.9	34.6	32.8	27.2	12.5	4.2	29.5	31.0	3.0	1.3	16.6
160.0 Deg	—1.0	—22.1	—29.3	—20.4	8.3	11.2	23.1	50.6	47.0	38.6	28.7	22.3	3.8	— 4.5	32.2	36.2	1.4	—0.5	16.6
165.0 Deg	—1.0	—26.4	—36.2	—25.1	7.5	6.9	19.0	57.4	59.0	42.8	22.5	10.0	— 5.9	— 8.8	32.8	37.2	— 1.3	—2.4	16.6
170.0 Deg	—1.0	—30.6	—42.9	—29.8	5.9	3.7	15.6	58.2	55.4	37.8	16.4	— 2.9	—14.3	—10.8	28.8	33.5	— 4.7	—4.3	16.6
175.0 Deg	—1.0	—34.5	—49.0	—34.7	3.4	4.2	17.5	54.6	38.9	21.6	11.3	— 9.5	—18.1	—12.2	18.6	26.2	— 8.2	—6.0	16.6
180.0 Deg	—1.0	—38.1	—54.3	—39.6	— 1.2	6.8	21.2	47.8	19.9	2.1	6.6	— 8.2	15.9	—13.9	7.0	17.2	—11.0	—7.4	16.6

TABLE II

Distribution of surface density $10^6\ G\sigma$ in m/s² (Rapp)

Theta	180	170	160	150	140	130	120	110	100	90	80	70	60	50	40	30	20	10	0
Phi																			
—175.0 Deg	—8.3	—38.1	—28.8	—14.8	—14.9	1.5	10.1	16.1	21.5	17.5	23.6	11.7	— 5.7	— 9.5	—15.1	— 1.5	— 0.5	—15.4	—6.0
—170.0 Deg	—8.3	—38.3	—31.7	—20.9	—19.1	— 4.9	— 0.0	9.5	12.0	4.2	22.1	23.7	— 3.7	—27.7	—28.9	— 1.4	0.7	—14.1	—6.0
—165. 0Deg	—8.3	—38.1	—35.1	—28.6	—25.3	—12.5	— 6.9	10.2	12.0	— 0.0	24.1	33.9	— 1.0	—39.1	—34.2	3.3	3.4	—12.5	—6.0
—160.0 Deg	—8.3	—37.6	—38.2	—35.7	—30.6	—16.5	— 8.5	15.4	17.8	3.3	25.2	37.4	3.5	—38.9	—29.5	11.3	6.7	—10.6	—6.0
—155.0 Deg	—8.3	—36.6	—40.4	—39.9	—32.0	—17.4	— 5.6	18.9	21.2	7.1	20.3	31.6	8.5	—29.3	—18.0	19.9	9.8	— 8.4	—6.0
—150.0 Deg	—8.3	—35.2	—40.9	—39.7	—28.0	—12.9	— 1.6	16.0	17.1	6.4	8.9	18.4	10.9	—17.6	— 6.2	25.7	11.9	— 6.1	—6.0
145.0 Deg	—8.3	—33.3	—39.6	—35.0	—19.6	— 7.2	— 0.2	7.1	7.1	2.4	— 4.1	2.6	7.4	—11.8	— 0.2	26.0	12.3	— 3.7	—6.0
—140.0 Deg	—8.3	—30.9	—36.5	—27.0	— 9.5	— 4.1	— 3.1	— 3.8	— 2.8	— 1.0	—13.8	—12.2	— 3.3	—15.4	— 2.6	19.9	10.9	— 1.3	—6.0
—135.0 Deg	—8.3	—28.1	—32.2	—17.9	— 1.1	— 5.6	— 9.2	—12.0	— 9.1	— 1.5	—18.8	—25.3	—19.7	—25.5	—11.0	8.4	7.9	1.1	—6.0
130.0 Deg	—8.3	—24.9	—27.2	—10.2	3.3	—10.5	—15.0	—15.4	— 9.1	— 0.1	—20.7	—37.0	—36.6	—34.2	—19.8	— 5.6	3.9	3.4	—6.0
—125.0 Deg	—8.3	—21.5	—22.1	— 5.6	3.1	—15.9	—17.4	—14.6	— 8.6	0.8	—20.8	—45.6	—47.5	—33.8	—23.2	—19.0	— 0.3	5.7	—6.0
—120.0 Deg	—8.3	—17.9	—17.4	— 5.1	— 0.8	—18.7	—15.2	—11.6	— 9.2	— 0.6	—19.3	—47.4	—47.9	—22.3	—19.3	—29.0	— 3.8	7.8	—6.0
—115.0 Deg	—8.3	—14.1	—13.4	— 8.3	— 6.8	—17.9	— 9.8	— 7.5	—10.6	— 5.2	—16.2	—70.0	—38.5	— 4.8	—10.1	—34.4	— 6.1	9.8	—6.0
—110. 0Deg	—8.3	—10.4	— 9.8	—13.7	—12.7	—14.5	— 4.1	— 2.1	—10.3	—12.5	—12.6	—24.3	—24.4	9.8	— 1.1	—35.6	— 6.8	11.6	—6.0
—105.0 Deg	—8.3	— 6.7	— 6.6	—19.4	—16.8	—10.4	— 0.9	4.2	— 6.0	—19.9	— 8.0	— 4.4	—11.8	13.9	3.2	—33.7	— 6.1	13.1	—6.0

TABLE II *(continued)*

Distribution of surface density $10^6\ G\sigma$ in m/s² (RAPP)

Theta	180	170	160	150	140	130	120	110	100	90	80	70	60	50	40	30	20	10	0
Phi																			
—100.0 Deg	—8.3	— 3.2	— 3.3	—23.1	—17.9	— 6.9	— 1.8	9.5	1.2	—23.4	— 4.0	15.3	— 3.9	6.7	0.9	—30.1	— 4.5	14.4	—6.0
— 95.0 Deg	—8.3	0.0	0.5	—23.5	—15.2	— 4.5	— 6.1	9.5	6.3	—20.0	5.0	30.9	0.2	— 5.7	— 5.6	—26.1	— 2.6	15.4	—6.0
— 90.0 Deg	—8.3	3.0	4.8	—19.9	— 9.3	— 2.2	—11.6	2.0	4.0	— 9.3	17.7	38.0	2.5	—14.9	—12.1	—22.5	— 1.0	16.0	—6.0
— 85.0 Deg	—8.3	5.6	9.6	—12.9	— 1.1	0.5	—14.5	—10.3	— 5.1	6.5	29.7	32.1	2.6	—15.9	—15.3	—19.8	— 0.3	16.3	—6.0
— 80.0 Deg	—8.3	7.8	14.5	— 3.8	7.2	3.9	—11.7	—18.9	—13.2	25.0	35.1	10.5	— 2.6	—10.4	—14.7	—18.7	— 1.0	16.3	—6.0
— 75.0 Deg	—8.3	9.4	19.0	5.4	13.7	7.0	— 2.5	—15.4	—10.4	43.5	30.7	—23.1	— 4.8	— 4.8	—12.9	—19.5	— 2.9	16.1	—6.0
— 70.0 Deg	—8.3	10.6	22.6	12.9	16.9	8.7	10.0	0.4	4.9	56.9	17.5	—57.4	—34.1	— 5.5	—12.8	—22.2	— 5.8	15.7	—6.0
— 65.0 Deg	—8.3	11.4	24.7	17.1	15.9	8.0	19.8	19.2	23.1	57.7	— 0.7	—78.6	—49.8	—13.3	—15.8	—26.1	— 9.1	15.2	—6.0
— 60.0 Deg	—8.3	11.6	25.2	17.4	11.1	5.1	22.1	28.5	30.2	40.4	—19.9	—78.3	—53.8	—22.9	—19.6	—29.7	—11.8	14.8	—6.0
— 55.0 Deg	—8.3	11.4	24.0	14.3	3.6	0.8	16.3	22.5	20.5	8.9	—37.1	—58.9	—41.8	—26.5	—21.4	—31.1	—13.1	14.5	—6.0
— 50.0 Deg	—8.3	10.9	21.3	9.0	— 5.0	— 4.0	6.1	6.2	1.8	—23.0	—49.1	—32.1	—18.3	—19.0	—16.8	—28.5	—12.0	14.4	—6.0
— 45.0 Deg	—8.3	10.2	17.8	3.2	—13.0	— 8.6	— 3.5	— 9.8	—12.7	—40.1	—53.1	—11.7	6.4	— 1.4	— 5.4	—21.2	— 8.3	14.6	—6.0
— 40.0 Deg	—8.3	9.3	13.9	— 1.2	—18.1	—12.8	— 9.8	—18.6	—16.7	—36.8	—47.8	— 5.3	22.4	20 1	10.0	— 8.5	— 1.6	15.1	—6.0
— 35.0 Deg	—8.3	8.5	10.2	— 2.6	—18.3	—16.0	—13.0	—20.8	—15.1	—20.9	—34.7	—10.3	26.4	37.7	24.7	5.0	7.4	15.8	—6.0
— 30.0 Deg	—8.3	7.9	7.2	— 0.5	—12.2	—16.7	—14.4	—20.7	—16.5	— 4.3	—17.0	—17.6	22.3	46.7	34.4	20.4	18.2	16.7	—6.0
— 25.0 Deg	—8.3	7.5	5.2	4.8	— 9.1	—13.1	—19.4	—19.9	—22.0	5.1	1.8	—18.7	13.3	47.7	37.2	34.7	29.4	17.5	—6.0
— 20.0 Deg	—8.3	7.4	4.3	11.8	15.2	— 4.7	—12.4	—16.9	—24.4	11.9	18.8	—11.0	20.5	44.2	34.4	46.3	39.8	18.3	—6.0
— 15.0 Deg	—8.3	7.8	4.5	12.3	31.6	6.5	— 9.0	—10.6	—17.1	21.0	31.7	1.6	30.1	41.9	28.0	54.0	48.1	18.9	—6.0
— 10.0 Deg	—8.3	8.7	5.6	22.4	42.0	16.2	— 6.5	— 4.2	— 2.7	32.8	38.8	13.8	43.3	43.5	24.3	57.3	53.4	19.1	—6.0
— 5.0 Deg	—8.3	10.1	7.7	22.9	43.7	20.6	— 6.9	— 2.5	8.2	41.1	44.3	23.0	54.0	48.0	21.8	55.9	55.1	18.8	—6.0
0.0 Deg	—8.3	12.0	10.6	20.0	36.3	18.5	— 8.7	— 6.0	7.1	38.7	47.0	29.8	57.2	52.1	21.5	49.9	52.9	18.1	—6.0
5.0 Deg	—8.3	14.3	14.4	15.1	22.7	12.6	— 7.9	— 9.0	— 5.1	23.5	48.0	34.4	50.8	52.8	21.8	39.8	47.3	17.0	—6.0
10.0 Deg	—8.3	16.9	19.1	10.7	8.4	7.3	— 1.0	— 4.7	—19.1	— 0.1	44.8	35.0	35.5	49.8	21.7	26.8	39.2	15.4	—6.0
15.0 Deg	—8.3	19.7	24.7	8.7	— 1.3	5.6	11.1	7.9	—25.7	—23.5	35.8	28.4	25.8	42.2	21.8	12.8	29.8	13.5	—6.0
20.0 Deg	—8.3	22.7	30.7	10.4	— 3.1	11.1	23.0	22.1	—22.0	—37.4	23.6	19.1	— 2.0	36.7	20.7	8.1	20.3	11.4	—6.0
25.0 Deg	—8.3	25.6	36.8	15.6	3.1	19.3	29.0	29.0	—11.8	—36.1	16.0	10.1	—11.9	35.3	21.7	— 9.1	12.2	9.2	—6.0
30.0 Deg	—8.3	28.3	42.5	23.0	14.4	28.0	27.0	24.6	— 1.9	—21.1	18.3	7.4	—11.7	39.0	24.4	—13.3	6.3	7.0	—6.0
35.0 Deg	—8.3	30.8	47.0	30.4	26.6	34.1	19.8	12.2	1.5	— 2.6	26.5	10.3	— 4.6	41.7	27.5	—12.2	3.2	4.9	—6.0
40.0 Deg	—8.3	32.8	58.1	35.8	35.9	35.6	11.8	— 1.2	— 4.1	5.7	29.2	11.7	2.8	41.9	29.3	— 6.8	2.6	2.9	—6.0
45.0 Deg	—8.3	34.4	51.3	38.1	40.4	32.2	5.4	— 9.9	—16.0	— 2.4	17.3	5.4	5.5	35.3	27.2	1.0	3.9	1.9	—6.0
50.0 Deg	—8.3	35.4	50.8	36.9	40.4	25.0	0.3	—11.5	—26.6	—20.8	— 6.8	— 8.1	2.8	21.3	20.0	8.4	6.2	— 0.8	— 6.0

TABLE II *(continued)*

Distribution of surface density $10^6\ G\sigma$ in m/s² (RAPP)

Theta	180	170	160	150	140	130	120	110	100	90	80	70	60	50	40	30	20	10	0
Phi																			
55.0 Deg	—8.3	35.8	48.7	33.0	37.6	16.4	— 3.9	— 6.8	—29.1	—36.4	—31.0	—21.9	— 9.2	3.7	7.5	13.2	8.3	— 2.5	—6.0
60.0 Deg	—8.3	35.7	45.5	27.6	34.1	9.5	— 6.2	2.0	—23.3	—42.8	—45.2	—29.0	— 6.4	—15.8	— 9.1	13.5	9.2	— 4.2	—6.0
65.0 Deg	—8.3	34.9	41.7	21.9	31.3	6.4	— 4.7	12.0	—18.1	—46.4	—49.6	—28.8	— 9.3	—33.4	—27.0	— 8.8	8.1	— 5.9	—6.0
70.0 Deg	—8.3	33.6	37.8	17.0	29.1	6.7	1.2	19.3	—23.9	—58.6	—52.0	—25.7	—11.9	—46.3	—42.1	— 9.2	4.8	— 7.7	—6.0
75.0 Deg	—8.3	31.8	34.2	13.4	26.8	7.8	7.8	20.4	—42.6	—81.6	—57.1	—24.0	—15.2	—54.1	—54.1	—11.9	— 9.4	— 9.4	—6.0
80.0 Deg	—8.3	29.4	31.0	11.4	23.7	6.3	8.9	12.8	—64.9	—102.4	—61.4	—24.2	—17.3	—49.1	—57.8	—24.7	— 6.8	—11.2	—6.0
85.0 Deg	—8.3	26.6	29.2	21.0	19.8	0.6	— 0.4	— 3.7	—76.5	—103.4	—58.3	—24.9	—16.4	—37.4	—53.8	—34.9	—13.7	—12.8	—6.0
90.0 Deg	—8.3	23.3	25.6	12.0	16.2	— 8.1	—12.6	—26.3	—69.9	—78.1	—47.1	—26.3	—13.0	—20.7	—44.2	—42.6	—19.9	—14.3	—6.0
95.0 Deg	—8.3	19.6	22.8	13.7	13.6	—16.5	—42.0	—49.0	—48.8	—36.3	—33.4	—30.1	—10.3	— 5.0	—32.4	—46.7	—24.6	—15.6	—6.0
100.0 Deg	—8.3	15.6	19.5	15.2	12.1	—21.8	—58.8	—63.9	—23.3	4.9	—22.1	—34.9	—11.6	3.6	—22.5	—47.9	—27.1	—16.7	—6.0
105.0 Deg	—8.3	11.2	15.3	15.5	10.5	—24.2	—61.6	—64.8	— 1.8	34.0	—10.5	—35.2	—16.5	2.6	—16.8	—44.1	—27.1	—17.4	—6.0
110.0 Deg	—8.3	6.7	10.0	13.7	6.9	—26.8	—54.0	—50.8	12.2	49.8	7.3	—24.7	—21.1	— 5.2	—15.6	—38.5	—25.5	—17.9	—6.0
115.0 Deg	—8.3	1.9	3.7	9.5	0.5	—33.0	—42.6	—28.7	13.6	55.6	32.0	— 3.6	—20.2	—13.2	—16.3	—31.9	—19.8	—18.1	—6.0
120.0 Deg	—8.3	— 2.8	— 3.3	3.0	— 8.0	—43.3	—35.1	— 8.1	13.5	53.8	54.9	19.8	— 11.0	—14.6	—16.8	—22.0	—13.6	—18.1	—6.0
125.0 Deg	—8.3	— 7.5	—10.7	— 4.8	—15.9	—53.4	—33.9	4.7	15.0	47.1	65.5	35.6	5.2	— 5.7	—15.1	—12.4	— 6.5	—17.8	—6.0
130.0 Deg	—8.3	—12.1	—17.9	—12.8	—20.5	—56.9	—34.7	10.6	14.4	40.7	61.5	39.2	24.0	7.7	—11.8	— 2.0	9.4	—17.7	—6.0
135.0 Deg	—8.3	—16.4	—24.1	—19.8	—20.5	—48.5	—30.6	15.4	21.9	40.6	50.3	34.4	39.3	21.7	— 6.7	6.0	6.6	—17.4	—6.0
140.0 Deg	—8.3	—20.4	—28.9	—25.0	—16.8	—32.1	—18.1	23.1	35.9	46.5	40.6	26.7	45.3	23.6	— 2.7	13.5	11.4	—17.3	—6.0
145.0 Deg	—8.3	—23.9	—32.0	—28.1	—12.3	—10.9	0.1	32.6	48.2	50.7	34.9	21.7	39.2	25.7	0.5	19.3	14.3	—17.2	—6.0
150.0 Deg	—8.3	—27.1	—33.2	—28.8	— 9.9	6.1	17.6	40.0	51.1	45.4	29.4	15.5	22.3	15.9	3.8	23.3	15.2	—17.2	—6.0
155.0 Deg	—8.3	—29.8	—32.9	—27.4	—10.7	14.2	29.0	43.1	45.0	32.0	28.2	7.4	1.1	6.3	8.8	25.1	14.3	—17.3	—6.0
160.0 Deg	—8.3	—32.0	—31.3	—24.1	—13.6	14.0	33.5	43.5	38.1	20.9	18.1	— 1.4	—16.4	2.8	15.2	24.5	11.9	—17.4	—6.0
165.0 Deg	—8.3	—33.9	—29.3	—19.8	—16.3	10.0	33.4	43.4	37.5	21.1	18.5	— 7.5	—24.3	5.8	20.7	21.3	8.5	—17.4	—6.0
170.0 Deg	—8.3	—35.5	—27.5	—15.3	—16.9	6.7	31.1	42.2	41.9	30.3	23.6	— 8.9	—22.7	13.4	21.6	15.9	4.9	—17.3	—6.0
175.0 Deg	—8.3	—36.6	—26.6	—12.2	—15.5	5.5	27.0	37.1	42.8	36.9	27.8	— 5.5	—15.9	15.2	15.2	9.1	1.8	—17.0	—6.0
180.0 Deg	—8.3	—37.5	—27.0	—11.8	—14.0	4.7	13.9	27.2	34.8	31.8	27.1	1.5	— 9.4	7.1	1.6	2.6	— 0.2	—16.4	—6.0

Appendix B

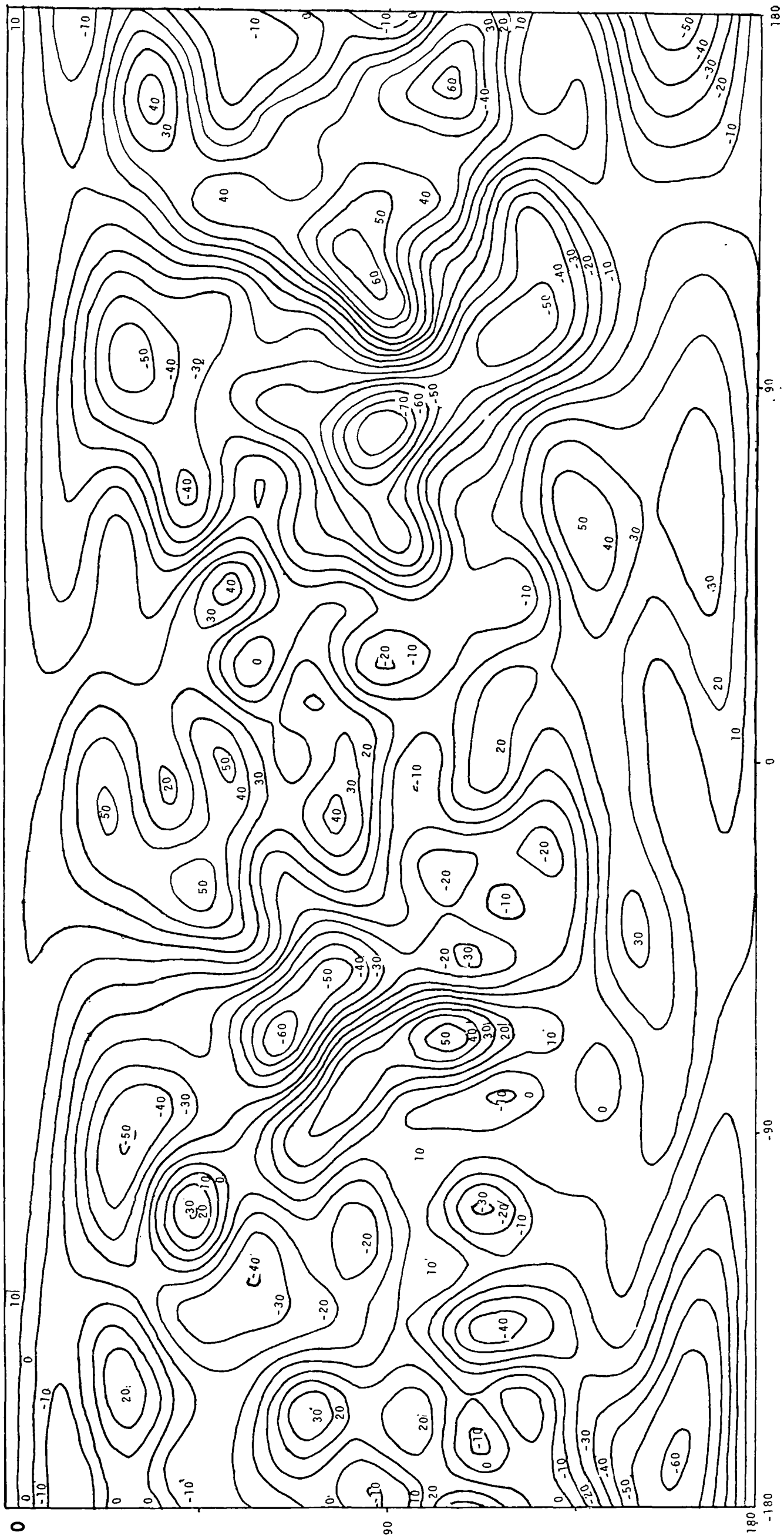

Fig. 1. Distribution of surface density $10^6\ G\sigma$ in m/s^2 (SAO).

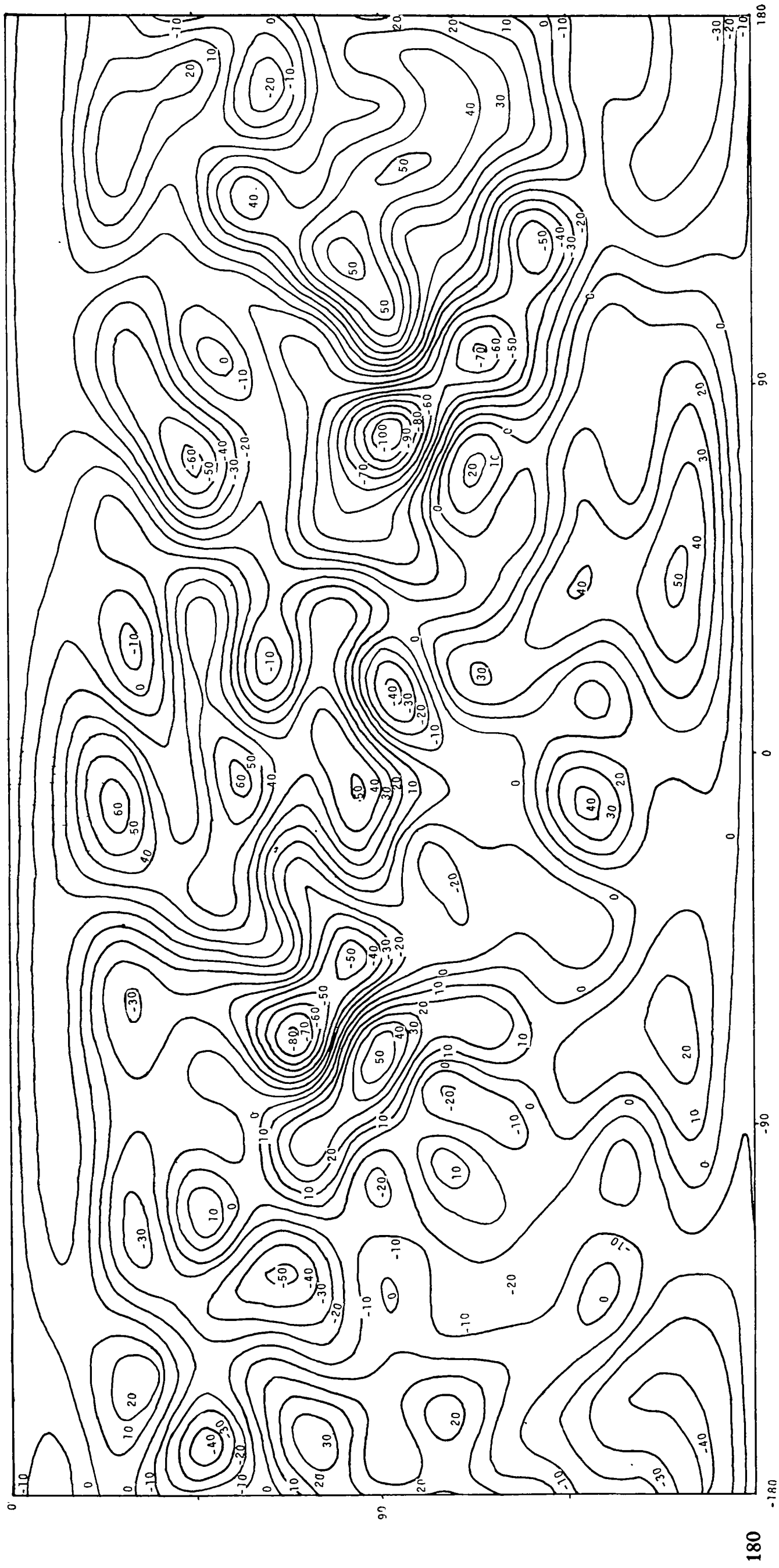

Fig. 2. Distribution of surface density $10^6\ G\sigma$ in m/s^2 (Rapp).